An Investigation of Residual Stress Gradient Effects in FIB-DIC Micro-Ring-Core Analysis

Enrico Salvati, Alexander J.G. Lunt, Tan Sui and Alexander M. Korsunsky*

***Abstract* — In many cases residually stresses surface layers that are obtained by surface treatment or coating deposition contain significant stress gradients. These gradients affect the performance of component surfaces under the conditions of contact loading in service, such as impact, scratch and abrasion, wear, erosion, fretting fatigue, etc. The determination of residual stress in the close vicinity of sample surfaces, at the depths ranging from sub-micron to a few microns, is a challenging task that cannot be accomplished routinely using existing techniques. A challenging aspect of the problem of stress evaluation concerns the nature of weighting of the contributions from different depths below the surface within the gauge volume. In the present study we focus our attention on this issue, specifically, on the effects of sub-surface stress gradients on the apparent stress value obtained by FIB-DIC micro-ring-core analysis. The implications of this investigation are discussed in the concluding section.**

***Index Terms*—Eigenstrain, FEM, FIB, Residual Stress**

I. Introduction

The evaluation of the residual stress at the microscopic scale can be accomplished using the semi-destructive ring-core drilling method [1]. The procedure involves the use of Focused Ion Beam (FIB) milling for the creation of an annular marker that creates a central pillar of stress-relieved material. Scanning Electron Microscopy (SEM) imaging of the pillar surface is used as input for Digital Image Correlation (DIC) analysis to determine the strain change (relief) as a function of the milling depth. The FIB milling procedure is carried out in a stepwise fashion, with DIC analysis performed at each stage in order to compute strain change. The comparison of the strain relief profile with a Finite Element Model (FEM) prediction allows the determination of the residual stress within the material volume defined by the pillar diameter and depth.

Manuscript received Dec 26, 2014; revised Jan 5, 2015. This work was supported in part by EU FP7project iSTRESS ‘’Pre-standardisation of incremental FIB micro-milling for intrinsic stress evaluation at the sub-micron scale”.

Enrico Salvati is doctoral student in the Department of Engineering Science, University of Oxford, OX1 3PJ, UK (e-mail: enrico.salvati@eng.ox.ac.uk).

Alexander J.G. Lunt is doctoral student in the Department of Engineering Science, University of Oxford, OX1 3PJ, UK (e-mail: alexander.lunt@chch.ox.ac.uk).

Tan Sui is post-doctoral researcher in the Department of Engineering Science, University of Oxford, OX1 3PJ, UK (e-mail: tan.sui@eng.ox.ac.uk).

*Alexander M. Korsunsky is Professor in Engineering Science at the University of Oxford, OX1 3PJ, UK (e-mail: alexander.korsunsky@eng.ox.ac.uk).

The above method (that can be referred to as the FIB-DIC micro-ring-core technique) is undergoing a period of active development, as part of the European pre-standardisation project iSTRESS. As part of this project, cross validation of the method against other techniques has been carried out in a number of studies [2,3,4]. Some of the validation techniques, such as micro-Raman spectroscopy, can work well even for amorphous materials. In contrast, micro-focus X-ray diffraction (particularly using synchrotron radiation) is limited to crystalline materials only. For such cases it offers an excellent validation approach, provided the material in question is (nano)poly-crystalline, which ensures the combination of coherent scattering with good grain statistics for the production of smooth powder diffraction patterns.

In the study reported in [4], an important practical question was raised. Whenever FIB-DIC micro-ring-core method is applied to coatings, it is important to consider the possibility that the residual stress within the coating varies with the depth from the surface. For example, coatings obtained by vapor deposition techniques contain residual stress depth profiles. These profiles depend strongly on the process parameters, as well as the substrate properties. This aspect is a critical issue for the design of structures in which residual stress can affect their performance. For example, when the coating is deposited using variable bias voltage, a smooth or stepwise variation in the residual stress state can be obtained [5].

Different methods applied for the analysis of such situations provide *average* measures of residual stress obtained from the sampling volume defined by the nature of the technique. However, the precise nature of averaging involved in each experimental configuration is not necessarily uniform, and must be carefully evaluated.

The elucidation of this phenomenon in the case of FIB-DIC micro-ring-core drilling method forms the subject of the present investigation. By using detailed FE modeling we quantify the dependence of the strain relief perceived at the pillar surface on the residual stress variation with the depth from the surface. FEM simulations performed allow the evaluation of the influence factors as a function of the milling step discretization. Additionally, simulations were conducted after imposing a linear residual stress gradient in a thin coating layer. The strain relief profile was evaluated for different gradient slopes whilst keeping the average value constant. The results are discussed and conclusions drawn.

II. The Eigenstrain Method of Residual Stress Analysis

Numerical simulations of residual stress states are conveniently conducted using the eigenstrain method [6]. This is by now a well-established method for direct and inverse stress analysis in solids. Using pseudo-thermal

ISBN: 978-988-19253-9-8
ISSN: 2078-0958 (Print); ISSN: 2078-0966 (Online)

expansion simulation, arbitrary eigenstrain profiles can be readily imposed. This task is readily accomplished by introducing a spatially varying thermal expansion profile that is given by

$$\bar{\bar{\varepsilon}}^*(z) = \bar{\bar{\alpha}}(z)\Delta T \quad (1)$$

Here $\bar{\bar{\alpha}}(z)$ is the position-dependent tensor of the coefficients of linear thermal expansion. It contains six independent parameters, which allows the imposition of any desired eigenstrain mode, including compression and expansion along selected axes, as well as shear. During computation this tensor is multiplied by the virtual temperature change, producing pseudo-thermal local strain. The temperature change can be conveniently set to unity for simplicity. Setting diagonal elements of tensor $\bar{\bar{\alpha}}(z)$ equal, and off-diagonal elements to zero corresponds to isotropic thermal expansion behavior.

The pseudo-thermal expansion eigenstrain model was implemented in Abaqus© by means of the UEXPAN subroutine.

III. Milling Step Influence Evaluation

A. Modelling

The axi-symmetric simulation carried out in this study used elastically isotropic material model, and isotropic (pseudo)thermal expansion behaviour. The geometry and the finite element mesh chosen for the model are illustrated in Figure 1.

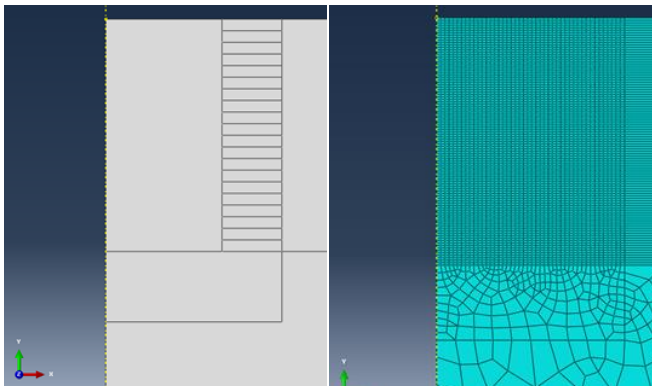

a) b)

Fig. 1. a) The model geometry and b) FEM discretization.

The fineness of the mesh in the depth direction was chosen to ensure smoothness of solution, and to allow discrete steps as small as 1/20th of the depth h=D. The milling process was simulated by setting the material properties of the milled region to be equal to those of air (Young's modulus E_{air}=0.001 MPa and Poisson's ratio ν_{air} =0.001). For the milling procedure composed of n steps, simulation steps were performed at normalized depths h/D ranging between zero and unity. At simulation step i, a constant expansionary (positive) eigenstrain value was imposed at milling depths between h/D=(i-1)/n and h/D=i/n. In this way, the presence of compressive residual stress was simulated. As output of the simulation, the strain at the pillar surface was monitored, and the average elastic strain computed. An additional FEM calculation was necessary in order to evaluate the elastic strain induced by eigenstrain in the condition where no milling has been done, in order to obtain the initial "unrelieved" strain value (i=0).

B. Results

A 3D representation of the stress field (Fig. 2b) illustrates the pillar deformation as a consequence of eigenstrain application (circled).

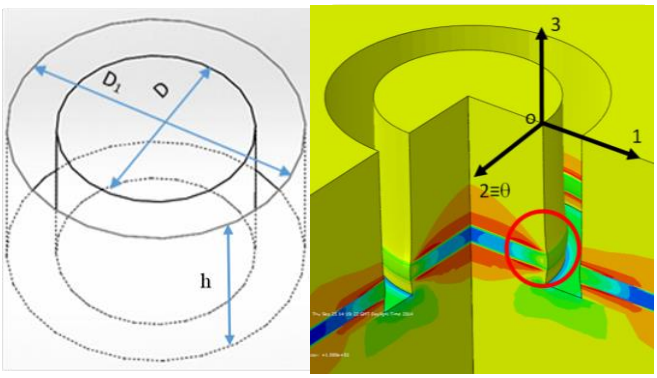

a) b)

Fig. 2. a) Micro-ring-core geometry. b) 3D representation and contour plot of the elastic hoop strain.

It is important to note that linear elastic simulation was used. This implies that any plastic deformation that may take place as a consequence of milling was ignored. This is an important assumption that needs to be verified in each individual case. For example, when hard ceramic coating layers are considered, plastic deformation is unlikely. In contrast, when the surface of a ductile metallic alloy is probed, this becomes a realistic possibility that needs to be taken into account. Provided the linearity of material response is assured, the net sum of individual eigenstrain step in terms of elastic strain at the surface has to be equal to the total stain relief in the case where the entire eigenstrain profile is applied through all the milling depth. In this way is possible to normalize the average elastic strain at the surface and obtain the fractional effect of each milling step on the final result. The graph below shows the normalized weights for the contribution of a constant equal eigenstrain "band" corresponding to a specific h/D value, where h is the milling depth, and D is the pillar diameter.

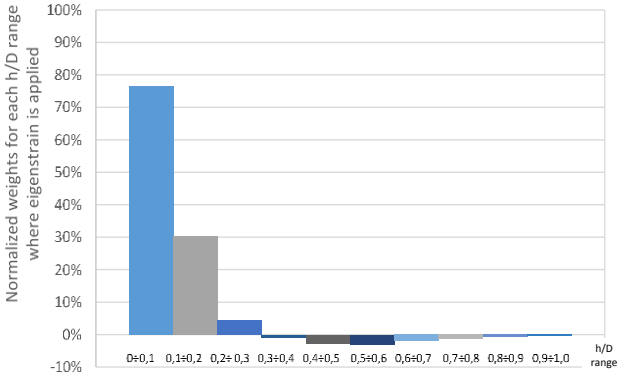

Fig. 3. The depth profile of weighting influence on the perceived surface strain relief, shown as percentage vs the normalized milling depth h/D.

ISBN: 978-988-19253-9-8
ISSN: 2078-0958 (Print); ISSN: 2078-0966 (Online)

The profile obtained in this study shows an interesting effect. At certain depths of milling, particularly at the *h/D* values around 0.3 – 0.8, the effect perceived at the surface is negative. This means that, for compressive residual stress imposed, the presence of residual stress at these depths induces compressive surface strain relief measured by DIC, as opposed to the expected expansion. This is competing with the strong expansion effect caused by the same compressive residual stress present at shallow depths. For example, the residual stress present in the very near surface layers of the material, at the depths characterized by the *h/D* ratio between zero and 0.1, contributed 76% to the total stain relief observed.

The "negative relief effect" can be explained by the hypothesis of non-uniformity of the pillar deformation: when a pillar of intermediate aspect ratio is "pinched" at the base, it causes expansion (rather than compression) at its free surface.

It is interesting to note the relationship between the weighting plot in Fig. 3, and the well-established strain relief vs depth profile. This profile has been derived from numerical simulations of the deformation induced in a residually stressed surface following micro-ring-core drilling, and is well described by the following "master function" [7]:

$$\varepsilon^* = 1.12\,\Delta\varepsilon^{\infty}\left(\frac{z}{1+z}\right)\left[1+\frac{2}{(1+z^2)}\right] \qquad (2)$$

where the depth parameter $z = \frac{h}{0.42\,D}$.

The nature of this function can be seen in Fig. 5, where the plot of strain relief under constant residual stress as a function of depth is shown for the case of $\gamma = 0$.

The consideration of incremental strain relief quickly leads to the conclusion about the relationship between the master function for strain relief under constant residual stress, and weighting plot of Fig 3. Namely, the weighting function corresponds to the *derivative* of the master function, which becomes negative around the *h/D* value of 0.4.

IV. Linear Residual Stress Gradient

A. Modelling

As mentioned before, many coating processes induce residual stress profiles that vary through the layer thickness. In fact, to the first approximation it is convenient to consider the case of linear gradient, with the maximum stress value present at the coating surface. In order to evaluate how the strain relief perceived in the FIB-DIC micro-ring-core method is affected by the presence of a gradient, the following computational procedure was adopted. Firstly, for the sake of simplicity, it was assumed that the residual strain profile is linear and compressive. Due to the linear nature of the phenomena studied, this does not represent a limitation. In order to provide a uniform basis for comparing different linear profiles, the average residual stress value throughout the coating layer was assumed to be constant. Obviously, this average value corresponds to the residual stress level at mid-depth of milling, i.e. *h/D* ratio of 0.5.

The eigenstrain method was used for the application of residual stress through the coating layer, as described in Figure 4. The average residual stress is noted in Figure as $< \sigma_{res} >$, and the maximum increment with respect to this value at the sample surface is denoted by $\sigma_{max} - < \sigma_{res} > = \sigma^+$. A non-dimensional parameter that quantifies the steepness of the gradient is given by:

$$\gamma = \frac{\sigma^+}{< \sigma_{res} >} \qquad (3)$$

The value of this parameter equal to unity corresponds to the case of residual stress dropping to zero at the interface between the coating and the substrate, and reaching double its average value at the coating surface.

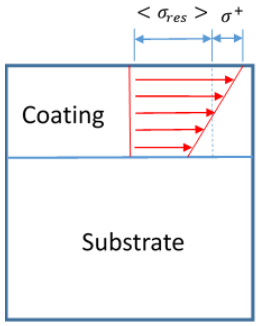

Fig. 4. Schematic representation of the analyzed model and residual stress profile applied

B. Results

Four cases were simulated that corresponded to different residual stress gradients. Since the shape of expected relief curve was similar to the one where no residual stress gradient are present, it was convenient to use varying depth step size in the simulation: in the first half of the entire milling depth, the simulation was conducted using the step size of *h/D*=0.05, while the second half was simulated using *h/D*=0.1. The relief curves were constructed on the basis of these calculations, and are shown in Fig. 5.

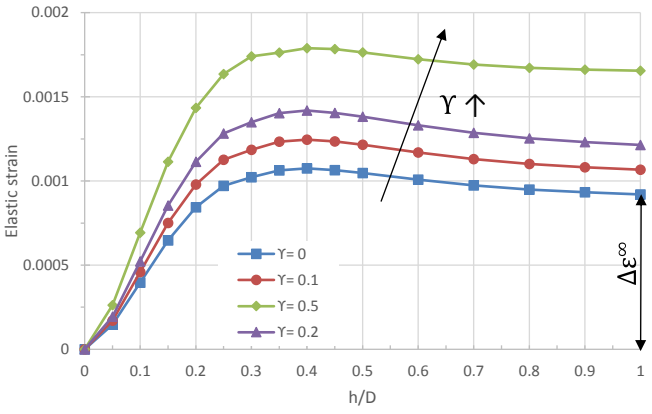

Fig. 5. Relief curves at different gradient slopes

The result shows how the apparent relief curves change as a function of the different gradient, whilst the mean stress value within the coating is kept constant. Even though the average residual stress imposed is unchanged, the perceived value at the stub ($\Delta\varepsilon^{\infty}$) surface increases, reflecting the increase in the surface stress value. As noted previously, the

ISBN: 978-988-19253-9-8
ISSN: 2078-0958 (Print); ISSN: 2078-0966 (Online)

stress values at the most shallow depths have the greatest influence on the final apparent strain relief at the pillar surface.

In order to evaluate the relationship between the residual stress gradient within the layer and the apparent residual stress value obtained by the FIB-DIC micro-ring-core method, the complete strain relief value was converted into stress. The assumption of plane stress as used, so that on the basis of known Young's modulus and Poisson's ratio of the coating, Hooke's law was used to evaluate the apparent residual stress. This value was normalised with respect to the *average* stress in the coating and plotted as shown in Fig. 6(a). The profile shows a steep variation characterised by the slope in excess of unity: the apparent stress calculated from FIB-DIC analysis grows even faster than the slope of stress gradient within the film. This somewhat paradoxical result arises as a consequence of the "pinching" effect.

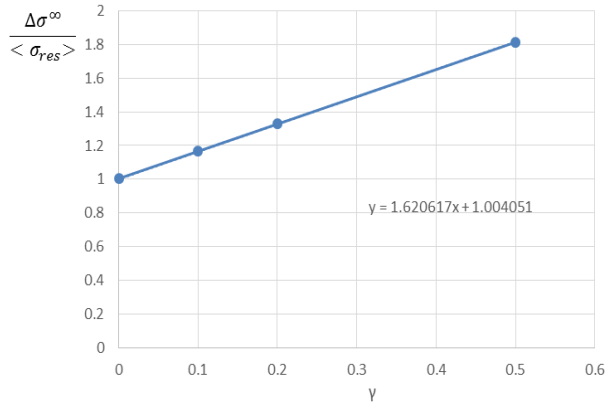

a)

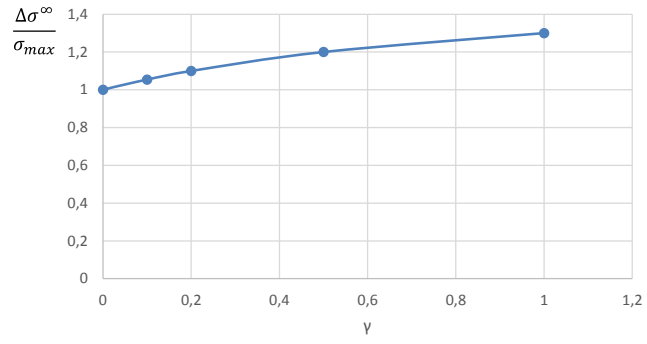

b)

Fig. 6. Relief curves at different gradient slopes plotted as (a) apparent stress (from FIB-DIC calculation) normalised by the *average* residual stress in the coating, and (b) apparent stress normalised by the stress value at the surface.

It has become clear from the foregoing discussion that it is the very near-surface values of stress that affect the apparent relief, and hence the FIB-DIC micro-ring-core evaluation. Therefore, in Fig. 6(b) the results were re-plotted in the form of apparent stress normalised with respect to the *surface* residual stress value, versus the normalised milling depth. The plot displays significantly smaller deviations from unity, suggesting a maximum deviation of only 30%, even for the case of very steep residual stress gradient within the coating given by γ=1. This value of γ corresponds to the situation when the stress drops to zero at the interface between the coating and substrate.

V. Conclusions

The results presented here were obtained from the study of the effect of non-constant residual stress profile existing in the near surface regions. The weighting function analysis has shown that the stress values at different depths make different contributions to the apparent residual stress value. It has been found that the depths up to h/D = 0.1 contribute 76% of the apparent value, whilst the influence of the depths h/D between 0.1 and 0.2 contribute around 30% of the apparent value. Therefore, in total the depths up to h/D = 0.2 contribute over 90% to stress evaluation using this technique. In contrast, for depths h/D>0.3 the contribution is almost null or even negative. It follows that judicious choice of the core pillar diameter can be useful in obtaining a perception of the residual stress variation. Nevertheless, depth profiling using this approach must be attempted with caution, since the deconvolution of influences of different depths, particularly in the presence of negative weights, and taking into account the influence of noise, may make the resulting mathematical problem ill-posed or unstable. These conclusions are supported by the results of the stress gradient effects on the analysis.

Acknowledgment

The authors express their gratitude to Zora Strelcova and Jiri Dluhos at TESCAN Brno, s.r.o., Czech Republic, for their ongoing advice and support in the operation of FIB-SEM facilities in the Multi-Beam Laboratory for Engineering Microscopy (MBLEM), Department of Engineering Science, University of Oxford, UK.

References

[1] A.M. Korsunsky, M. Sebastiani, E. Bemporad. *Focused ion beam ring drilling for residual stress evaluation.* Materials Letters 63, 1961-1963, (2009).

[2] N. Baimpas, E. Le Bourhis, S. Eve, D. Thiaudière, C. Hardie, A.M. Korsunsky. *Stress evaluation in thin films: Micro-focus synchrotron X-ray diffraction combined with focused ion beam patterning for d_0 evaluation*. Thin Solid Films 549, 245-250 (2013).

[3] N. Baimpas, A.J.G. Lunt, I.P. Dolbnya, J. Dluhos A.M. Korsunsky. *Nano-scale mapping of lattice strain and orientation inside carbon core SiC fibres by synchrotron X-ray diffraction*. Carbon 79, 85-92 (2014).

[4] E. Bemporad, M. Brisotto, L.E. Depero, M. Gelfi, A.M. Korsunsky, A.J.G. Lunt, M. Sebastiani. *A critical comparison between XRD and FIB residual stress measurement techniques in thin films*. Thin Solid Films 574, 224-231 (2014).

[5] R. Daniel, E. Jager, J. Todt, J B. Sartory, C. Mitterer, J. Keckes. *Mono-textured nanocrystalline thin films with pronounced stress-gradients: On the role of grain boundaries in the stress evolution*. Journal of Applied Physics 115, 203507 (2014).

[6] A.M. Korsunsky. *Eigenstrain analysis of residual strains and stresses*, Journal of Strain Analysis 44, 29-43 (2009).

[7] A.M. Korsunsky, M. Sebastiani, E. Bemporad. Residual stress evaluation at the micrometer scale: *Analysis of the thin coating by FIB milling and digital image correlation*. Surface and Coating Technology, 205, 2393-2403 (2010)